

The Influence of friction Force on Modified Gear Teeth and its Effect on Bearing Forces

S.S.Ghosh

Department of Mechanical Engineering
Indian Institute of Technology, Kharagpur
Kharagpur, India
ghoshss123@gmail.com

G.Chakraborty

Department of Mechanical Engineering
Indian Institute of Technology, Kharagpur
Kharagpur, India
goutam @ mech.iitkgp.ernet.in

Abstract— Theoretical analysis of vibration of a geared system becomes quite complicated because of the presence of several factors contributing to generation of the excited motions. Some examples are static transmission error (STE), gear tooth flexibility, backlash, friction forces present at the contact surfaces, torsional and flexural rigidity of the shafts on which gears are mounted etc. Considerations of all these factors make a model too complicated to be treated analytically. STE is believed to be chiefly responsible for gear vibration and noise. Consequently, tooth profile modification is employed to minimize dynamic transmission error (DTE) variation and dynamic load. However, high performance gears are still noisy in many applications. One possible explanation is the presence of friction as a noise source. A six degree-of-freedom torsional-translational model is considered to study the effect of friction in the line-of-action (LOA) and off-line-of-action (OLOA) direction under gear tooth modification. An attempt is made to find optimum profile modification for minimum bearing force along LOA and OLOA direction.

Keywords—*sliding friction, profile modification, dynamic force, bearing force*

I. INTRODUCTION

Gear noise has always been concern for the designers and manufacturers of geared systems due to its significant influence on the performance of the overall system and also due to imposition of stringent noise regulations and standards. In majority of the gear models, friction forces are neglected compared to the normal forces, acting along the direction of common normal to the contacting gear teeth. Fluctuation of normal force causes dynamic transmission error (DTE) which is usually assumed to be chiefly responsible for gear vibration and noise. Normally tooth profile modification is employed to minimize TE variation and dynamic load. However, gear designed with minimum TE variation does not always show intended noise reduction [1]. The effect of friction force which acts perpendicular to the normal force, cannot be completely ignored. During gear meshing, the gear and pinion undergo a rolling and sliding action, except at the pitch point, where pure rolling takes place. Since, rolling resistance is

considerably smaller than sliding resistance, its contribution to the total tooth friction is usually ignored. Also, the sliding friction forces are small compared to the transmitting force. Consequently the friction force has been ignored in the earlier gear dynamic models. When noise was considered in the gear system, it was gradually understood that the effect of tooth friction should be considered in the gear dynamic model.

The effect of friction on torsional dynamics was studied by Radzimovsky et al. [2] for a four-square test rig. Iida et al. [3] estimated the response in the tooth sliding direction due to friction force, while response in other direction was ignored. The possibility of gear noise excitation by tooth friction was quantitatively discussed by Borner et al. [1], who found that it can be a crucial parameter for structure-borne vibration. Vedmer et al. [4] analyzed off-line-of-action (OLOA) effects in spur gearing and also included tooth friction in their torsional dynamic model. Houser et al. [5] experimentally demonstrated that the frictional force plays pivotal roles in determining the load transmitted to the bearing and the housing in the OLOA direction, the effect being more prominent at higher torque and under low speed conditions. Velex et al. [6] described an iterative procedure to evaluate the effect of sliding friction, the tooth shape variations and time-varying mesh stiffness in spur and helical gears and compared with measurements. Lundvall et al. [7] considered profile modification and manufacturing errors in a multi-degree-of-freedom spur gear model and examined the effect of sliding friction on angular dynamic motions. They reported that the profile modification has less influence on dynamic transmission error (DTE) when friction effects were included. He et al. [8] considered a multi-degree-of-freedom model incorporating time-varying sliding friction and realistic mesh stiffness with tip relief of gears. They showed that the sliding friction primarily excited the motion along OLOA direction and tip relief introduced amplification of the motion and forces along OLOA direction due to an out of phase relationship between normal load and friction forces. However,

the effect of different profile modification and finding the condition of optimum profile modification for minimum dynamic responses along LOA and OLOA directions when both static transmission error and frictional excitation are present, have not been considered so far. Dynamic mesh force, bearing force in LOA direction, bearing force in OLOA direction are considered to be important factors in the design of spur gear considering strength, durability and noise. In this study, an attempt is made to find optimum profile modification to achieve minimum noise (i.e. bearing force) and maximum strength of the teeth (i.e. minimum dynamic mesh force).

II. MATHEMATICAL MODEL OF THE SYSTEM

A multi-degree-of freedom torsional-translational model is considered in this study. The model is similar to one already established by He et al. [8]. A few features are introduced in this model, namely, backlash is added in the equation of motion, profile modification is added in the static load sharing model as Tavakoli et al. [9], time-varying co-efficient of friction, which will be discussed later, is introduced at each contact point along the line of action.

A pair of gears is modeled (Fig.1) using two disks (1 represents pinion and 2 represents gear) coupled by a non-linear spring having mesh stiffness (K_t) and a mesh damping (coefficient C_t). The mesh stiffness and mesh damping depend on individual gear pair (of stiffness $k_1(t), k_0(t)$ and damping co-efficient $c_1(t), c_0(t)$), as discussed below. The clearance element due to backlash ($2b_b$) is also introduced in the model. The resilient elements of supports are described by stiffness co-efficient k_{1x} and k_{2x} for the pinion and gear respectively in LOA direction, k_{1y} and k_{2y} for the pinion and gear respectively in OLOA direction. The corresponding damping coefficients are $c_{1x}, c_{2x}, c_{1y}, c_{2y}$, respectively. Motions of the system are described by rotational angles θ_1 and θ_2 , displacements by x_1 and x_2 in LOA direction and y_1, y_2 in OLOA direction of the center of the disks.

The model takes into account the influence of torque T_1 and T_2 on the pinion and gear shaft, respectively. A displacement function $\epsilon_p(t)$ is also applied along the direction LOA to model manufacturing error, assembly error. The effect of profile modification is provided by the load distribution model.

For a low contact ratio ($1 < CR < 2$) spur gear pair, two meshing teeth pairs need to be modeled for the

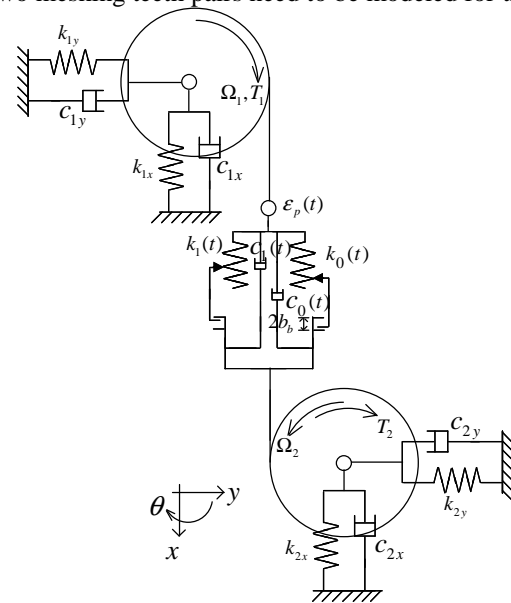


Fig. 1 Six-degree-of-freedom spur gear system

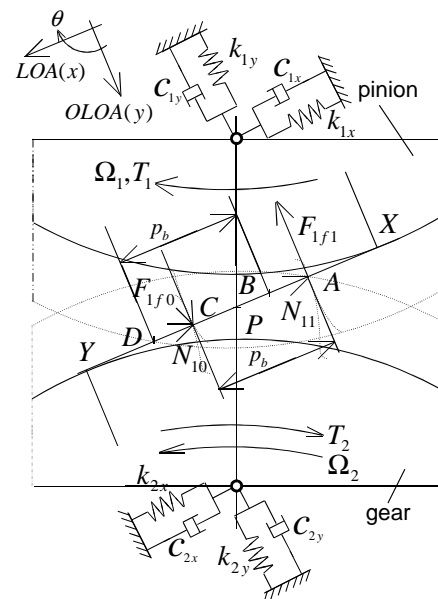


Fig. 2. Forces on gear teeth at the starting of a mesh cycle ($t = 0$)

construction of stiffness function. Fig.2 is a snapshot of the gear system at the starting ($t = 0$) of the mesh cycle. At that time, pair #1 (the tooth pair moving along line AC) just comes into mesh at point A and pair #0 (the tooth pair moving along line CD) is in contact at point C, which is the highest point of single tooth contact (HPSTC) of the pinion. When tooth pair #1 approaches the lowest point of single tooth contact (LPSTC) at point B, pair #0 leaves contact at point D. BC is the region of single tooth contact. Further, at the pitch point P, between B and C, the relative sliding velocity of the pinion with respect to gear will be reversed, resulting in reversal of friction force. The

contact distance along the line of action is represented by time. Key timings for the meshing events are t_m , t_b and t_p representing meshing time, time for contacting at LPSTC of the pinion (point B in Fig. 2) and time for contacting at the pitch point (point P) respectively. The timings can be calculated as

$$t_m = \frac{P_b}{\Omega_1 R_{b1}}, t_b = t_m \cdot \frac{L_{AB}}{P_b}, t_p = t_m \cdot \frac{L_{AP}}{P_b} \quad (1)$$

where Ω_1 is the nominal pinion speed, R_{b1} is the base radius of the pinion, P_b is the base pitch, L_{AB} is the length AB (Fig. 2) and L_{AP} is the length AP (Fig. 2). The stiffness function of the i -th meshing tooth pair $k_i(t)$ can be calculated from the mesh stiffness function $K_i(t)$ for a single tooth pair rolling through the entire meshing process at any time instant as,

$$k_i(t) = K_t \left[(1-i)t_m + \text{mod}(t, t_m) \right], \quad i = 0, 1 \quad (2)$$

where “mod” is the modulus function defined as :
 $\text{mod}(x, y) = x - y \text{ floor}(x/y)$, if $y \neq 0$.

Here “floor” is the floor function and $\text{floor}(x/y)$ means the lower integer of x/y value.

The mesh damping co-efficient $c_i(t)$ is assumed to be time-varying and is related to $k_i(t)$ by a constant damping ratio ξ_m as follows:

$$c_i(t) = 2\xi_m \sqrt{k_i(t) J_e}, \quad i = 0, 1. \quad (3)$$

Here, $J_e = J_1 J_2 / (J_1 R_{b2}^2 + J_2 R_{b1}^2)$

and J_1, J_2 are the moment of inertias of pinion and gear respectively.

The normal forces acting on pinion and gear are

$$N_{1i} = -N_{2i} = k_i(t) f \left[R_{b1} \theta_1 - R_{b2} \theta_2 - \varepsilon_p + x_1 - x_2 \right] + c_i(t) \left[R_{b1} \dot{\theta}_1 - R_{b2} \dot{\theta}_2 - \dot{\varepsilon}_p + \dot{x}_1 - \dot{x}_2 \right] \quad (4)$$

Here ε_p is the unloaded static transmission error.

The friction forces are considered to be proportional to the normal tooth forces, as per Coulomb friction law. So, $|F_f| = |\mu N|$, where μ is the sliding friction coefficient. The direction of F_f is determined from the calculation of the normal relative sliding velocity. Then, with reference to Fig. 2, which shows forces acting only on pinion, the frictional forces on pinion and gear are,

$$\left. \begin{aligned} F_{2f0}(t) &= \mu N_{20}(t) \\ F_{2f1}(t) &= \mu N_{21}(t) \text{sgn} \left[\text{mod}(\Omega_1 R_{b1} t, P_b) - L_{AP} \right] \end{aligned} \right\} \quad (5)$$

$$\left. \begin{aligned} F_{2f0}(t) &= \mu N_{20}(t) \\ F_{2f1}(t) &= \mu N_{21}(t) \text{sgn} \left[\text{mod}(\Omega_2 R_{b2} t, P_b) - L_{AP} \right] \end{aligned} \right\} \quad (6)$$

where “sgn” is the sign function. The moment arm of the friction forces for the pinion and gear of 0-th and first pair are given by

$$\left. \begin{aligned} \rho_{10} &= L_{XA} + P_b + \text{mod}(\Omega_1 R_{b1} t, P_b) \\ \rho_{11} &= L_{XA} + \text{mod}(\Omega_1 R_{b1} t, P_b) \end{aligned} \right\} \quad (7)$$

$$\left. \begin{aligned} \rho_{20} &= L_{YC} - \text{mod}(\Omega_2 R_{b2} t, P_b), \\ \rho_{21} &= L_{YC} + P_b - \text{mod}(\Omega_2 R_{b2} t, P_b) \end{aligned} \right\} \quad (8)$$

where L_{XA} is the length XA, L_{YC} is the length YC, Ω_1 and Ω_2 are the nominal speed of the pinion and gear respectively and R_{b2} is the base radius of the gear.

A. Equations of motion for six-degree-of-freedom system

The co-ordinate system is chosen in this model is such that one of the axes (x axis) is parallel to LOA as shown in Fig. 1, while y axis is that to OLOA direction. The equation of motion of the six-degree-of-freedom model, shown in Fig. 1, can be written as,

$$J_1 \ddot{\theta}_1 + (k_0(t) + k_1(t)) f(R_{b1} \theta_1 - R_{b2} \theta_2 - \varepsilon_p + x_1 - x_2) R_{b1} + (c_0(t) + c_1(t)) (R_{b1} \dot{\theta}_1 - R_{b2} \dot{\theta}_2 - \dot{\varepsilon}_p + \dot{x}_1 - \dot{x}_2) R_{b1} + \rho_{10} \mu N_{10} + \rho_{11} \mu N_{11} \text{sgn}[\text{mod}(\Omega_1 R_{b1} t, P_b) - L_{AP}] = T_1 \quad (9)$$

$$J_2 \ddot{\theta}_2 - (k_0(t) + k_1(t)) f(R_{b1} \theta_1 - R_{b2} \theta_2 - \varepsilon_p + x_1 - x_2) R_{b2} - (c_0(t) + c_1(t)) (R_{b1} \dot{\theta}_1 - R_{b2} \dot{\theta}_2 - \dot{\varepsilon}_p + \dot{x}_1 - \dot{x}_2) R_{b2} + \rho_{20} \mu N_{20} + \rho_{21} \mu N_{21} \text{sgn}[\text{mod}(\Omega_2 R_{b2} t, P_b) - L_{AP}] = -T_2 \quad (10)$$

$$m_1 \ddot{x}_1 + c_{1x} \dot{x}_1 + k_{1x} x_1 + N_{10} + N_{11} = 0 \quad (11)$$

$$m_2 \ddot{x}_2 + c_{2x} \dot{x}_2 + k_{2x} x_2 + N_{20} + N_{21} = 0 \quad (12)$$

$$m_1 \ddot{y}_1 + c_{1y} \dot{y}_1 + k_{1y} y_1 - \mu N_{10} - \mu N_{11} \text{sgn}[\text{mod}(\Omega_1 R_{b1} t, P_b) - L_{AP}] = 0 \quad (13)$$

$$m_2 \ddot{y}_2 + c_{2y} \dot{y}_2 + k_{2y} y_2 - \mu N_{20} - \mu N_{21} \text{sgn}[\text{mod}(\Omega_2 R_{b2} t, P_b) - L_{AP}] = 0 \quad (14)$$

The dynamic transmission error (DTE) along LOA direction is given by

$$\delta(t) = R_{b1} \theta_1 - R_{b2} \theta_2 + x_1 - x_2 \quad (15)$$

The dynamic bearing forces on pinion shaft in LOA and OLOA direction respectively are given by

$$\begin{aligned} F_{1Bx} &= k_{1x} x_1 + c_{1x} \dot{x}_1, \\ \text{and } F_{1By} &= k_{1y} y_1 + c_{1y} \dot{y}_1. \end{aligned} \quad (16)$$

Similarly, the dynamic bearing forces on gear shaft

in LOA and OLOA direction respectively are given by

$$F_{2Bx} = k_{2x}x_2 + c_{2x}\dot{x}_2,$$

and

$$F_{2By} = k_{2y}y_2 + c_{2y}\dot{y}_2. \quad (17)$$

B. Friction co-efficient model

The co-efficient of friction may be time-varying and time-invariant. For time-varying model, at each contact position of the gears, the load W' (unit load for each contact segment that represents a contact point) along the line of contact, is calculated. The friction models require maximum Hertzian Pressure, p_h , radii of curvature, surface velocities, component of sliding and rolling velocities in the direction normal to the contact line, slide to roll ratio etc. for each contact point. For a pair of gear in mesh, one contact point is equivalent to the contact between two virtual cylinders in contact. For double tooth contact load, sliding velocities, rolling velocities etc. are found out for each contact position and co-efficient of friction are found out for each tooth and for every contact position. Co-efficient of friction also depends upon absolute viscosity of lubrication oil, surface roughness. These parameters may be changed to cover various operating conditions for finding the effect of bearing forces in LOA and OLOA directions. Three friction models are used in the present work to find coefficient of friction. They are:

- i. Constant co-efficient of friction (μ) model
- ii. Benedict and Kelly model [10] and
- iii. Xu et al. model [11]

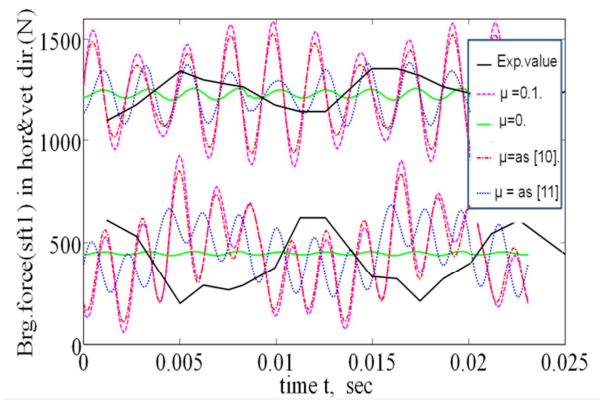
III. RESULT AND DISCUSSION

First, the gear system as used by Vexel et al. [8] is used here for the study. The basic parameters of this gear pair are listed in Table I. No backlash is assumed to exist in the gear system, hence, non-linear mesh spring may be considered as linear spring with time-varying mesh stiffness. The combined bearing shaft stiffness both k_{1x} and k_{1y} for the pinion shaft in the LOA and OLOA directions are taken to be 3.45×10^7 N/m, while k_{2x} and k_{2y} for the gear shaft are as 7.38×10^7 N/m. The damping ratios in each case are taken as 0.005. The involute profile deviation is taken as less than 5μ m. Both gears have symmetrical linear short tip relief of 20μ m over 20 percent of the active profile. All the data are taken from [6].

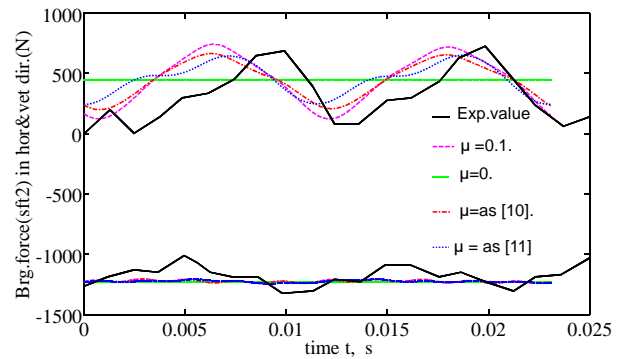
The gear mesh stiffness is calculated as discussed by Cornell [12]. The damping ratio is taken as 0.1 for the calculation of mesh damping. Using three friction models, the bearing forces along horizontal

TABLE I. PARAMETERS OF SPUR GEAR PAIR USED FOR MODEL VALIDATION, TAKEN FROM [6]

Centre distance, mm	366	
Tooth surface roughness(R_a), μ m	0.8	
Lubricant Viscosity at 40 ⁰ C, CP	82	
Variables	Pinion	Gear
No. of teeth	26	157
Module, mm	4	4
Pressure angle, degree	20	20
Shaft diameter(external), mm	70	90
Shaft length(Brg. To Brg.), m	0.64	0.64



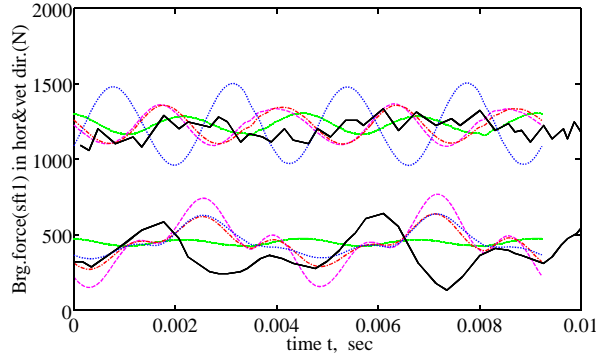
(a)



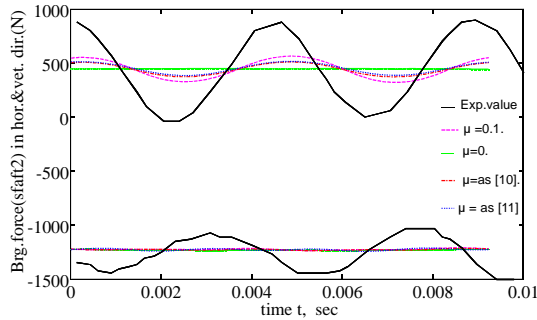
(b)

Fig. 3(a). Bearing forces in horizontal and vertical direction at the pinion shaft (sft1). Upper curves are for vertical force, lower curves are for horizontal force. Fig. 3(b). Bearing forces in horizontal and vertical direction at the gear shaft (sft2). Upper curves are for horizontal force, lower curves are for vertical force.

and vertical direction at pinion and gear shaft are calculated by solving the equations (9) to (14) using MATLAB and compared with the experimental results given by Vexel et al. [6]. The comparison is shown in Fig. 3(a) & 3(b) for 200 rpm and in Fig. 4(a) & 4(b) for 500 rpm. The simulation results capture the trend of experimental results as shown in Fig. 3 and Fig. 4.



(a)



(b)

Fig. 4(a). Bearing forces in horizontal and vertical direction at the pinion shaft (sft1). Upper curves are for vertical force, lower curves are for horizontal force. Fig. 4(b). Bearing forces in horizontal and vertical direction at the gear shaft (sft2). Upper curves are for horizontal force, lower curves are for vertical force.

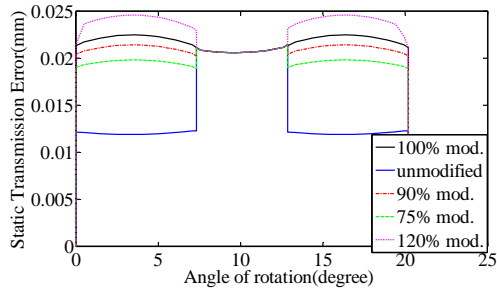


Fig. 5(a). STE curve for unmodified and modified gear teeth.

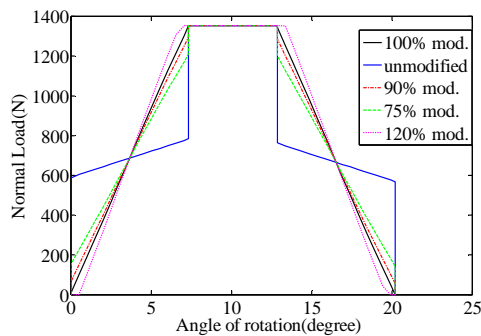


Fig. 5(b). Static normal tooth load curve for unmodified and modified gear teeth.

Next, basic spur gear pair used by He et al. [8] was used for the study of the effect of profile modification, friction and bearing forces. The design parameters of this pair are listed in Table II. Here also no backlash is assumed in the gear system. The combined bearing shaft stiffness both k_{1x} and k_{1y} for the pinion shaft in the LOA and OLOA directions are taken as 2.26×10^7 N/m, while k_{2x} and k_{2y} for the gear shaft are estimated as the same [8]. The damping ratios for each case are taken as 0.005.

Static transmission error (STE) curves and static tooth load sharing curves for unmodified and modified gear pair are shown in Fig. 5(a) and 5(b), dynamic transmission error and dynamic mesh force for unmodified and modified gear tooth are shown in Fig. 6(a) and 6(b). The effect of profile modification on dynamic load at different speed and load was shown by Lin et al. [13]. The amount of

TABLE II. PARAMETERS OF SPUR GEAR PAIR USED FOR OPTIMISATION, TAKEN FROM [8]

Centre distance, mm	88.9	
Tooth surface roughness(R_a), μm	0.1	
Lubricant Viscosity at 40°C , CP	10	
Variables	Pinion	Gear
No. of teeth	28	28
Module, mm	25.4/8	25.4/8
Pressure angle, degree	20	20
Face width, mm	6.35	6.35
Outside diameter, mm	94.94	94.94
Root diameter, mm	79.73	79.73

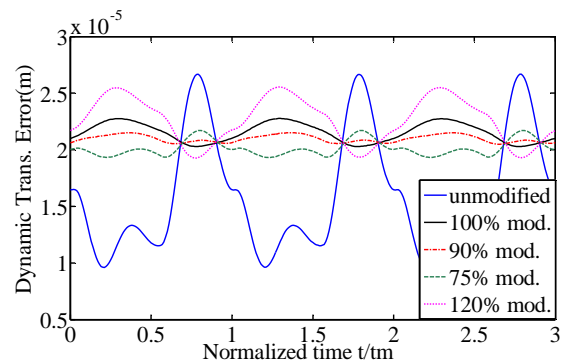


Fig. 6(a). DTE curve for unmodified and modified gear teeth.

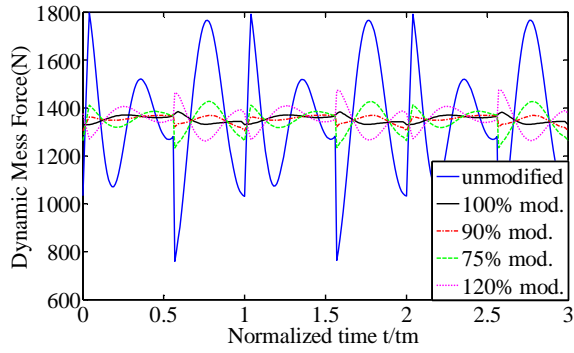
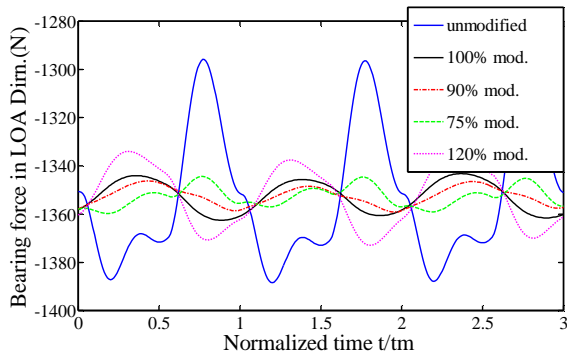


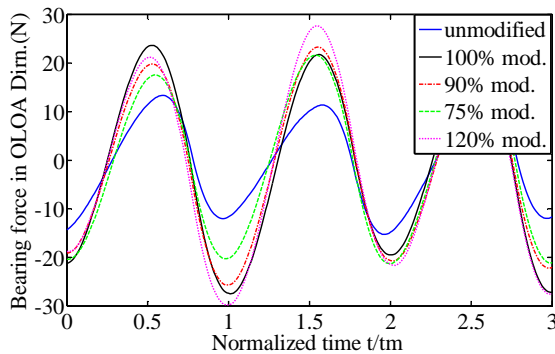
Fig. 6(b). Dynamic mesh force curve for unmodified and modified gear teeth.

profile modifications are normalized with respect to minimum amount of conventional tip relief. Welbourn stated that the minimum tip relief should be equal to twice the maximum spacing error plus the combined tooth deflection evaluated at the highest point of single tooth contact (HPSTC) [14].

Translation along LOA and OLOA direction at rotational speed of 5000 rpm of pinion shaft are shown in Fig. 7(a) and 7(b) for unmodified and modified gear teeth. Bearing forces in LOA and OLOA direction at the same rpm are shown in Fig.

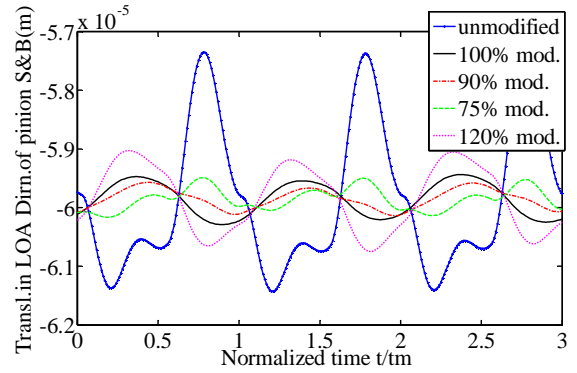


(a)

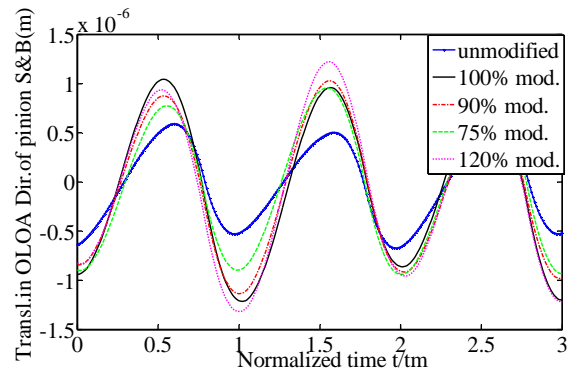


(b)

Fig. 7. Translation of pinion shaft and bearing (a) in LOA and (b) in OLOA direction.

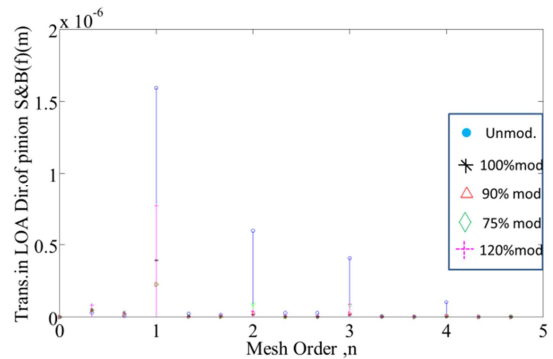


(a)

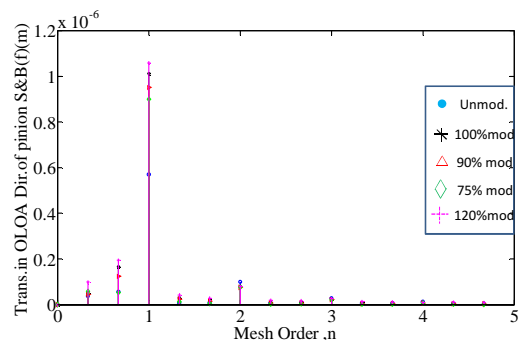


(b)

Fig.8. Bearing force of pinion shaft and bearing (a) in LOA and (b) in OLOA direction.



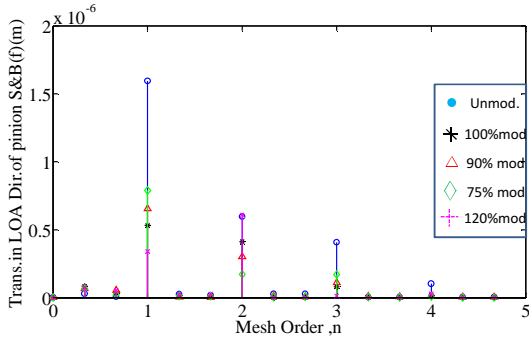
(a)



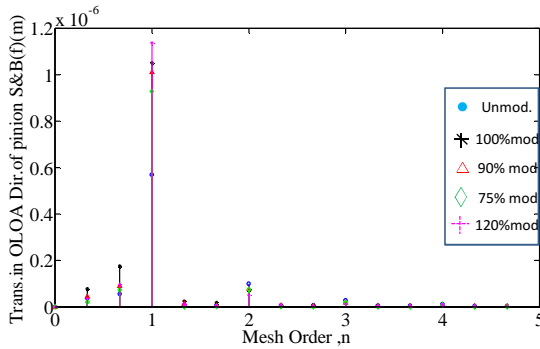
(b)

Fig. 9. Frequency spectrum of translation (a) in LOA and (b) in OLOA direction of pinion shaft and bearing of Fig. 7(a) and 7(b).

$\Omega_1 = 5000$ rpm, $\mu = 0.035$, $\mathcal{E}_p = 0$, linear tooth tip relief.

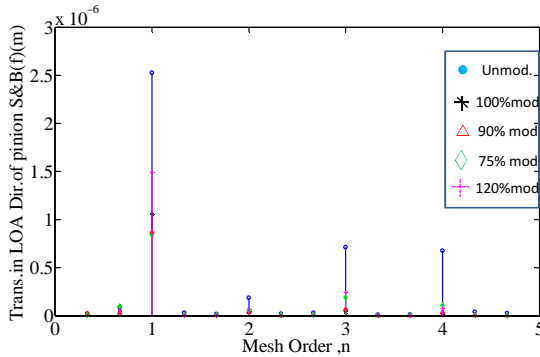


(a)

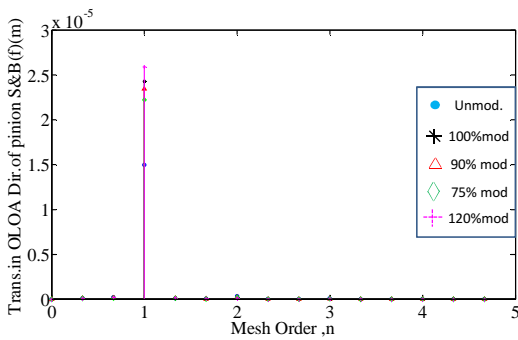


(b)

Fig. 10. Frequency spectrum of translation (a) in LOA and (b) in OLOA direction of pinion shaft and bearing. $\Omega_1 = 5000$ rpm, $\mu = 0.035$, $\mathcal{E}_p = 0$, parabolic tooth tip relief.

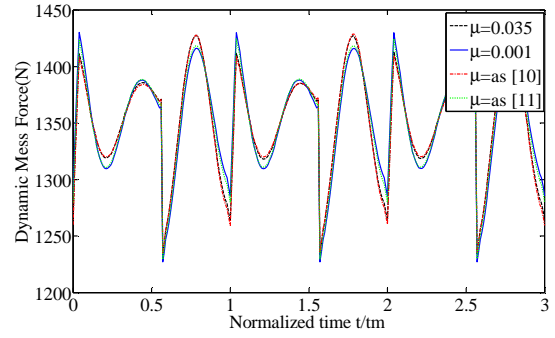


(a)

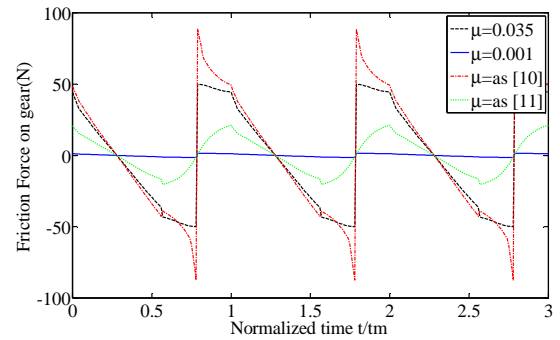


(b)

Fig. 11. Frequency spectrum of translation (a) in LOA and (b) in OLOA direction of pinion shaft and bearing. $\Omega_1 = 3000$ rpm, $\mu = 0.035$, $\mathcal{E}_p = 0$, linear tooth tip relief.

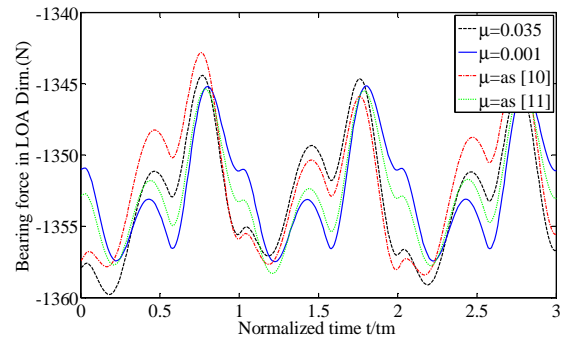


(a)

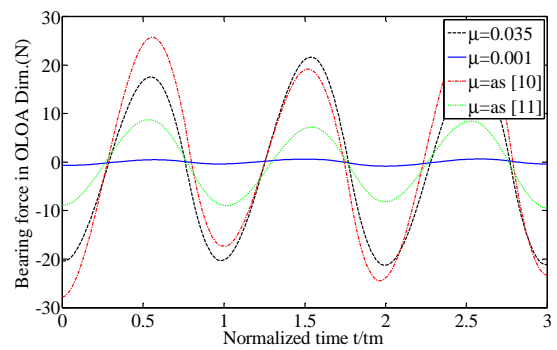


(b)

Fig. 12(a) and 12(b). Dynamic mesh force and friction force on gears at 5000 rpm of pinion with 75 percent tip relief with different μ values.



(a)



(b)

Fig. 13. Bearing force (a) in LOA and (b) in OLOA direction at 5000 rpm of pinion with 75 percent tip relief with different μ values.

8(a) and 8(b). From the figure, it is clear that translation and bearing force along LOA and OLOA direction are of same nature. Frequency spectrum of translation motion of Fig. 7 (a) and 7(b) are shown in Fig. 9(a) and 9(b). From the figure, it is clear that first harmonic plays predominant role in translation along the LOA and OLOA direction at 5000 rpm. It can also be observed that by providing 100 percent linear modification, the amplitude of the first harmonic decreases drastically in LOA direction while it increases along OLOA direction. Providing 75 percent linear modification will result in lower first harmonic amplitude in LOA as well as OLOA direction relative to other modifications. The situation is same for 3000 rpm of the pinion shaft, as shown in Fig. 11(a) and 11(b). Figure 10(a) and 10(b) show frequency spectra of translation along LOA and OLOA direction of pinion shaft and bearing rotating at 5000 rpm when parabolic tip relief is provided on both the gears. For parabolic tooth tip relief, the decrease of amplitudes of harmonics in LOA direction is relatively less and increase in harmonics in OLOA direction is more, indicating superiority of the linear tooth tip relief over parabolic tooth tip relief.

The effect of friction on dynamic mesh force and friction forces on gear teeth are shown in Fig. 12(a) and 12(b). The co-efficient of friction values are taken as 0.001 (approximately no friction), 0.035, as [10] and as [11]. The dynamic mesh forces are approximately the same in all cases. Friction forces are approximately same for Hz, peak to peak value of bearing forces in LOA direction do not change much with various Hz, peak to peak value of bearing forces in LOA direction do not change much with various $\mu = 0.035$ and as per Benedict et al. except near the pitch point. Friction force and co-efficient of friction is minimum with the consideration of Xu et al. . Surface roughness plays an important role in co-efficient of friction. Friction forces change their directions two times in a mesh cycle. However, change of magnitude of friction force is drastic at the pitch point. Bearing forces in LOA and OLOA direction are shown in Fig. 13(a) and Fig. 13(b) with different co-efficient of friction. As expected, peak to peak value of bearing force in LOA direction is maximum and peak to peak value of bearing force in OLOA direction is minimum for $\mu = 0.001$. The effect of coefficient of friction on peak to peak value of bearing force along OLOA direction is more.

Variation of peak to peak value of bearing forces along LOA and OLOA direction against mesh frequency are shown in Fig. 14 and 15 for various gear tooth modifications. Time-varying friction forces are calculated as suggested by Benedict and Kelly. From Fig. 15, it can be observed that bearing force along OLOA direction (indicating the effect of friction) at higher speed (say, 2500 Hz) is insignificant. Peak to peak value of the bearing

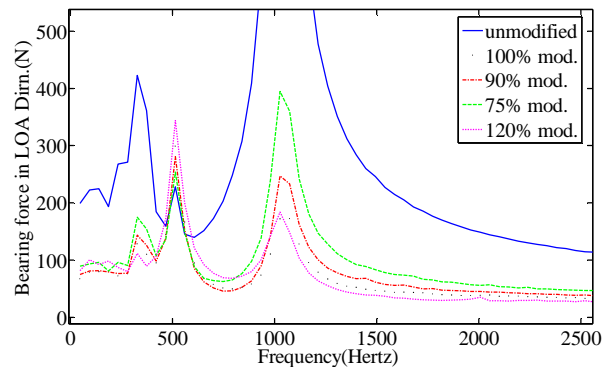


Fig. 14. Peak to peak value of bearing forces in LOA direction vs. mesh frequency at various tooth modification.

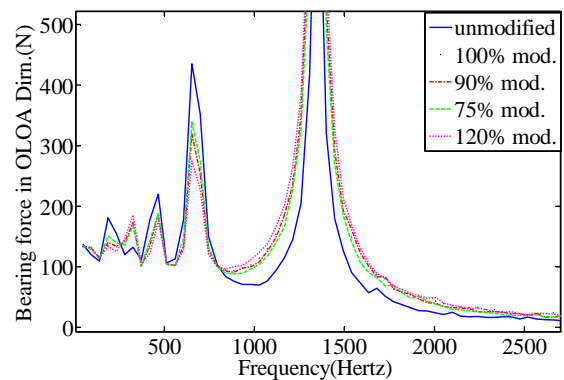
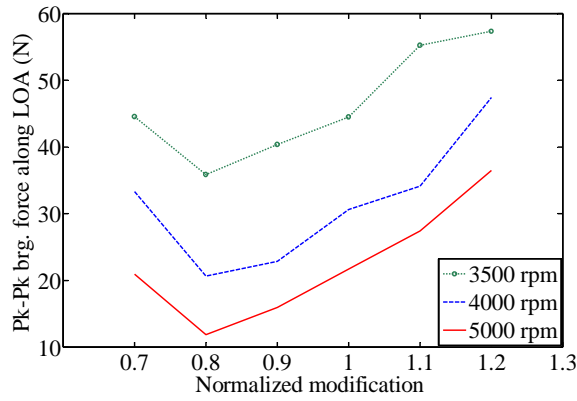


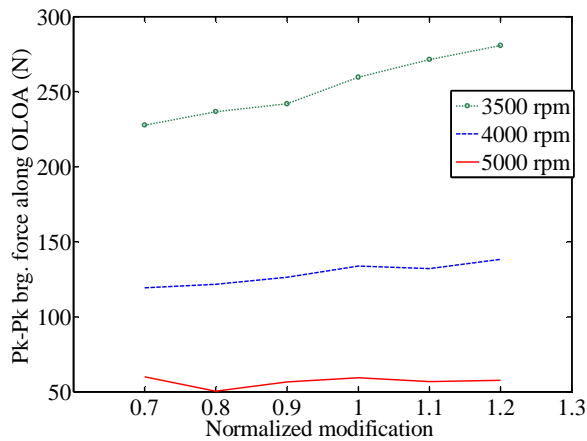
Fig. 15. Peak to peak value of bearing forces in OLOA direction vs. mesh frequency at various tooth modification.

force along OLOA direction is minimum for unmodified teeth above 800 Hz. Also bearing force along OLOA direction is minimum for 75 percent modification (among the numerical simulation done for 75% to 120% modification) above 800 Hz. Peak to peak value of bearing forces in LOA direction is more for 75% modification than other modifications above 800 Hz. However, above 1600 Hz, peak to peak value of bearing forces in LOA direction do not change much with various modifications. Hence, for higher mesh frequency operation of the gear teeth 75 to 80 percent normal tip relief may be effective for less bearing force in LOA as well as OLOA direction and consequently less noise in the gear system.

This point is clear from specific speed consideration as shown in Fig. 16(a) and 16(b). At 5000 rpm of the pinion, peak to peak bearing force in LOA and OLOA direction is minimum for 80 percent modification. For 4000 and 3500 rpm, peak to peak bearing force in LOA direction is minimum for 80 percent modification, while peak to peak bearing force in OLOA direction is minimum for 70 percent modification. However, dynamic mesh force is the first criterion for the design of spur gear. For the present case, the gear system running at



(a)



(b)

Fig.16(a). Peak to peak bearing force in LOA direction vs. normalized modification. Fig. 16(b). Peak to peak bearing force in OLOA direction vs. normalized modification.

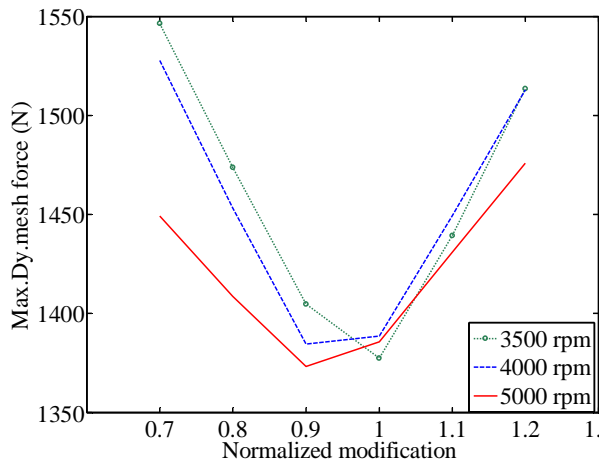


Fig. 17. Maximum dynamic mesh force vs. normalized modification.

the three speeds, maximum dynamic mesh forces are minimum for a profile modification between 90 to 100 percent as shown in Fig.17. Hence, some judicial adjustment should be done for profile modification in consideration with strength, durability and noise of spur gear system.

IV. CONCLUSIONS

A six-degree-of-freedom torsional-translational system is considered in this study to find the bearing forces in LOA and OLOA direction with unmodified and modified teeth. It is found that peak to peak value of the bearing forces in OLOA direction increases after modification at higher mesh frequencies. For the chosen geared system, it has been observed that 75 to 80 percent linear tip modification may be used for optimum modification considering bearing forces at higher speed of the gear. However, dynamic force is minimum for 90 to 100 percent modification. So, profile modification should be selected according to the importance of strength, durability and noise of spur gear.

REFERENCES

- [1] J. Borner and D. R. Houser, "Friction and Bending Moments on Gear Noise Excitations," SAE Trans. , 105, No. 6, pp. 1669-1676, 1996.
- [2] E. L. Radzimovsky, A. Miraferi, and W. E. Broom, "Instantaneous Efficiency and Coefficient of Friction of an involute Gear Drive," ASME J. Eng. Ind. , 95, pp. 1131-1138, 1973.
- [3] H. Iida, A. Tamura, and Y. Yamada, "Vibrational characteristics of friction between gear teeth," JSME Bull. , 28, pp. 1512-1519, 1985.
- [4] L. Vedmar and B. Henriksson, "A General approach for determining Dynamic Forces in Spur Gears," ASME J. Mech. Des. , 120, pp. 593-598, 1998.
- [5] D. R. Houser, M. Vaishya, and J. D. Sorenson, "Vibro-acoustic effects of friction in gears: an experimental investigation," SAE paper No. 2001-01-1516, 2001.
- [6] P. Velez and V. Cahouet, "Experimental and numerical investigations on the influence of tooth friction in spur and helical gear," Journal of Mechanical Design, ASME Trans. , 122(4), 515-522, 2000.
- [7] P. Lundvall, N. Stromberg, and A. Klarbring, "A flexible multi-body approach for frictional contact in spur gears," Journal of Sound and Vibration, 278, 3, pp. 479-499, 2004.
- [8] S. He, R. Gunda, and R. Singh, "Effect of sliding friction on the dynamics of spur gear with realistic time-varying stiffness," Journal of Sound and Vibration, 301, pp. 927-949, 2007.
- [9] M. S. Tavakoli and D. R. Houser, "Optimum Profile modification for the Minimization of Static Transmission Error of spur Gear," Journal of Mechanisms, Transmissions, and Automation in Design, ASME Trans. , 108, pp. 86- 94, 1986.
- [10] G. H. Benedict and B. W. Kelly, "Instantaneous Coefficient of Gear Tooth Friction," ASLE Trans. , 4, pp. 59-70, 1961.
- [11] H. Xu, A. Kahraman, N. E. Anderson, and D. G. Maddock, "Prediction of Mechanical Efficiency of Parallel - Axis Gear Pairs, Journal of Mechanical Design, ASME Trans. , 129, 1, 58-68, 2007.
- [12] R. W. Cornell, "Compliance and Stress sensitivity of Spur Gear Teeth," Journal of Mechanical Design, ASME Trans. , 103, 447-459, 1981.
- [13] H. H. Lin, F. B. Oswald, and D. P. Townsend, "Profile modification to Minimize spur Gear Dynamic Loading," Proc. of ASME 5th Int. Power Trans. And Gearing Conf. , Chicago, Illinois, Vol. 1, pp. 455-465, 1989.
- [14] D. B. Welbourn, "Fundamental Knowledge of Gear Noise-A survey," Proc. of I. Mech. E. Conf. on Noise and Vibration of Engines and Transmissions, Cranfield Institute of Tech. , July 1-11, 1979.